Tensile Behavior of a New Single Crystal Nickel-Based Superalloy (CMSX-4) at Room and Elevated Temperatures

A. Sengupta, S.K. Putatunda, L. Bartosiewicz, J. Hangas, P.J. Nailos, M. Peputapeck, and F.E. Alberts*

Tensile behavior of a new single-crystal nickel-based superalloy with rhenium (CMSX-4) was studied at both room and elevated temperatures. The investigation also examined the influence of γ' precipitates (size and distribution) on the tensile behavior of the material. Tensile specimens were prepared from single-crystal CMSX-4 in [001] orientation. The test specimens had the [001] growth direction parallel to the loading axis in tension. These specimens were given three different heat treatments to produce three different γ' precipitate sizes and distributions. Tensile testing was carried out at both room and elevated temperatures. The results of the present investigation indicate that yield strength and ultimate tensile strength of this material initially increases with temperature, reaches a peak at around 800 °C, and then starts rapidly decreasing with rise in temperature. Both yield and tensile strength increased with increase in average γ' precipitate size. Yield strength and temperature correlated very well by an Arrhenius type of relationship. Rate-controlling process for yielding at very high temperature ($T \geq 800$ °C) was found to be the dislocation climb for all three differently heat-treated materials. Thermally activated hardening occurs below 800 °C whereas above 800 °C thermally activated softening occurs in this material.

Keywords
nickel superalloy, single crystal, temperature, tensile behavior

1. Introduction

SINGLE-CRYSTAL nickel-based superalloys are used extensively in many high-temperature applications such as gas turbines, nuclear reactors, etc. These alloys have the best combination of elevated-temperature properties of any structural material.[1-3] These alloys exhibit a stress-rupture resistance superior to conventional polycrystalline superalloys at high temperatures. The single-crystal alloys have higher incipient melting temperatures than the polycrystalline superalloys. The absence of grain boundaries, which often act as crack initiation sites in these alloys, provides significant enhancements in thermal-fatigue resistance. These remarkably high fatigue properties also result from the absence of significant residual γ/γ' eutectic phase, carbides, oxides, nitride or sulfide inclusions, and microporosity when hot isostatic pressing (HIP) is used. In addition, presence of refractory alloying elements (tungsten, rhenium, and tantalum) and the absence of grain-boundary strengthening elements (boron, carbon, and zirconium) has a beneficial effect by providing high thermal fatigue resistance for these alloys.[4,5]

CMSX-4 is a recently developed material. It is a rhenium-containing second-generation ultrahigh-strength single-crystal superalloy initially developed for small gas turbines.[6] It is strengthened by the solid solution strengthening effects of chromium, tungsten, rhenium, and tantalum. The presence of aluminum and titanium provides additional strength due to precipitation-hardening effect of γ' phase. Small rhenium clusters (approximately 1 nm in size) were detected in this alloy.[6,7] These clusters act as powerful obstacles against dislocation movement in the γ matrix compared to the isolated solute atoms in solid solution and play a significant role in improving the strength of this alloy. This alloy has better stress-rupture temperature endurance than the first-generation CMSX alloys.[6,7] It has superior molten-salt hot-corrosion (sulfidation) characteristics and is an attractive candidate for complex single-crystal components that require exposure to very high temperature fabrication.[6,7] The effect of the reduced level of chromium in this alloy is offset by the increased aluminum content and by the presence of rhenium, which also increases oxidation resistance and decreases significantly the γ' coarsening kinetics.[8,9]

Both γ' precipitate size and distribution can significantly influence the mechanical properties of the single-crystal nickel-based superalloys at room and elevated temperature. The present studies were undertaken to examine the influence of γ' precipitate (size and distribution) on the various mechanical properties of CMSX-4 at both room and elevated temperatures. The earlier studies by these investigators[9] examined the growth kinetics of γ' precipitate and influence of γ' (size and distribution) on fatigue crack growth rate and fatigue threshold at both room and elevated temperatures. The present investigation is a continuation of the aforementioned study where the in-

A. Sengupta, Graduate Research Assistant, Department of Materials Science and Engineering, Wayne State University, Detroit, Michigan; **S.K. Putatunda,** Associate Professor, Department of Materials Science and Engineering, Wayne State University, Detroit, Michigan; **L. Bartosiewicz,** Staff Scientist, Scientific Research Laboratories, Ford Motor Co., Dearborn, Michigan; **J. Hangas,** Research Scientist, Scientific Research Laboratories, Ford Motor Co., Dearborn, Michigan; **P.J. Nailos,** Laboratory Engineer, Central Laboratory, Ford Motor Co., Dearborn, Michigan; **M. Peputapeck,** Laboratory Engineer, Scientific Research Laboratory, Ford Motor Co., Dearborn, Michigan; **F.E. Alberts,** Research Staff, Scientific Research Laboratory, Ford Motor Co., Dearborn, Michigan.
* Current address: VELTEC Laboratories, Taylor, MI

Table 1 Chemical Composition of CMSX-4

Element	wt.%
Chromium	6.5
Cobalt	10.0
Molybdenum	0.6
Tungsten	6.5
Tantalum	6.5
Rhenium	3.0
Aluminum	5.5
Titanium	1.0
Hafnium	0.1
Nickel	bal

fluence of γ' precipitate (size and distribution) on yield, tensile strength, and strain hardening exponent has been examined at both room and elevated temperatures.

2. Experimental Procedures

2.1 *Material*

The material used in this investigation is the single-crystal nickel-based superalloy CMSX-4. The single crystals of the alloy were provided by Cannon-Muskegon Corporation in the form of rods of diameter 12.5 mm (½ in.) and 150 mm (6 in.) long with axis parallel to [001] direction. The chemical composition of the material is given in Table 1. This alloy was cast in [001] orientation. The orientation of the cast alloy was verified using the back-reflection Laue method. The crystal was grown using a modified Bridgemann technique.[10]

2.2 *Specimen Preparation for Tensile Testing*

For tensile testing, round cylindrical tensile specimens were prepared following ASTM standard E-8.[11] The specimens were fabricated by the electrical discharge machine. The tensile direction in these specimens was in the [001] direction. Specimens had cylindrical gage sections measuring 25.4 mm (1 in.) long and 6.25 mm (0.25 in.) in diameter.

2.3 *Heat Treatments*

After fabrication, the specimens were given three different heat treatments. These are identified as heat-treated conditions A, B, and C. Condition A was obtained after solution treatment, of as-cast bar, in several stages, followed by high-temperature aging at 1080 °C for 4 h, followed by air cooling, and then finally by aging at 871 °C for 20 h, and finally air cooling. The details of these heat treatments are given in Table 2. This heat treatment has resulted in an average γ' size of 0.3 μm.[9] For condition B, heat-treated condition A specimens were further heat treated in the following way: The specimens, after heat treatment A, were aged at 1140 °C for 6 h, then air cooled. This was followed by aging at 871 °C for 100 h. Then, they were finally air cooled. This resulted in an average γ' size of 0.5 μm.[9] For condition C, specimens after heat treatment A were solution treated at 1290 °C for 4 h and then air cooled. This was followed by solution treatment for 2 h at 1290 °C, followed by water quench and then by two-step aging: aging at 1080 °C for 4 h, with air cooling, followed by final aging at 871 °C for 1000 h, with final air cooling, as shown in Table 2. This resulted in an average γ' precipitate size of 0.9 μm.[10,11] The volume fraction of γ' precipitates were determined using SEM and was found to be on the order of 70% in these specimens. The microstructures of these heat-treated specimens in heat-treated conditions A, B, and C are shown in Fig. 1(a), (b), and (c), respectively. The γ' precipitates obtained by these heat treatments were cuboidal[10,11] in nature.

Table 2 Heat Treatment Procedure

Heat-Treated Condition A: As-received bars solution treated at 1276 °C for 2 h, at 1287 °C for 2 h, at 1296 °C for 3 h, at 1304 °C for 3 h, at 1315 °C for 2 h, at 1321 °C for 2 h, at 1324 °C for 2, then finally air cooled
High-temperature aging at 1080 °C for 4 h, then air cooled, final aging at 871 °C for 20 h, then finally air cooled
Resultant γ' size = 0.30 μm, range = 0.25 to 0.35 μm

Heat-Treated Condition B: Two-step aging (after heat-treated condition A), aged at 1140 °C for 6 h, then air cooled, final aging at 871 °C for 100 h, then finally air cooled
Resultant γ' size = 0.50 μm, range = 0.4 to 0.5 μm

Heat-Treated Condition C: After heat-treatment A, 1290 °C for 4 h, then air cooled, solution treated at 1290 °C for 2 h, followed by water quench, then high-temperature aging at 1080 °C for 4 h, then air cooled, final aging at 871 °C for 1000 h, then finally air cooled
Resultant γ' size = 0.9 μm, range = 0.8 to 1.1 μm

2.4 *Tensile Testing*

Tensile tests were carried out in a Tinius Olsen* machine with SATEC F6** furnace attachment. The specimens were mounted on specially designed grips. The furnace was brought to the required temperature, and specimens along with the grips were introduced inside and properly mounted at both ends. Once the specimens attained the required temperature, the test was conducted. The strain rate was maintained 0.005 in./in./min up to yield and 0.05 in./in./min after yielding. Load and extension were recorded directly on a *X-Y* recorder. The temperature of the furnace was controlled within ±2 °C by a temperature controller. Three identical specimens were tested at each temperature, and the average values from three test samples are reported in Fig. 2 and 3 and Tables 3 to 5.

3. Results and Discussion

3.1 *Influence of γ' Precipitate Size on Yield Strength and Tensile Strength*

Typical stress-strain diagrams at room temperature indicate that the tensile curve increases initially and then flattens out after reaching the ultimate tensile strength. The tensile curves for all three γ' precipitate sizes were similar in nature. The elastic modulus of the material in room temperature was found to be 134 GPa. This value is within the range of values of other single-crystal nickel-based superalloys in this orientation. Figures 2 and 3 report the yield and tensile strengths of the material in heat-treated conditions A, B, and C as a function of tempera-

*Tinius Olsen Testing Machine Company, Inc., P.O. Box 429, Willow Grove, PA 19090-0429

**SATEC, 900 Liberty St., Grove City, PA 16127-9005

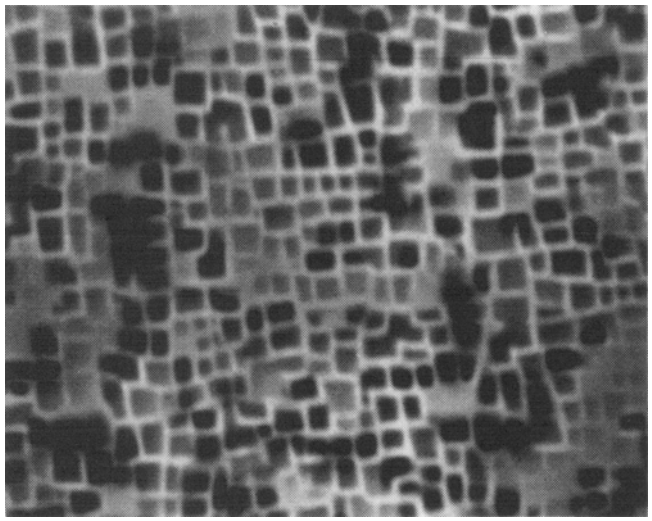

(a)

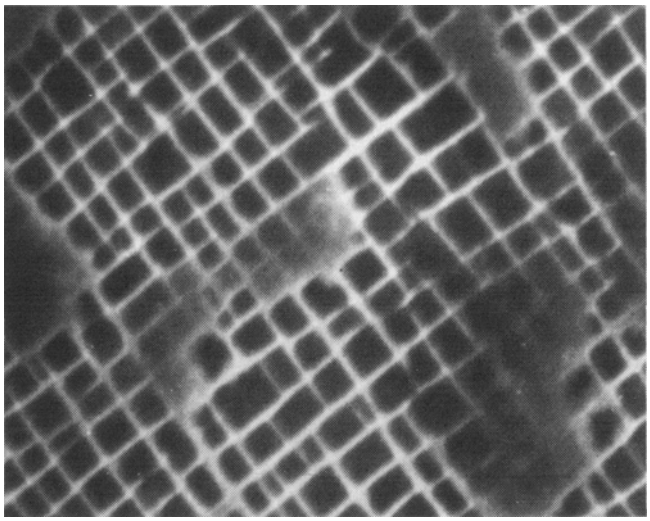

(b)

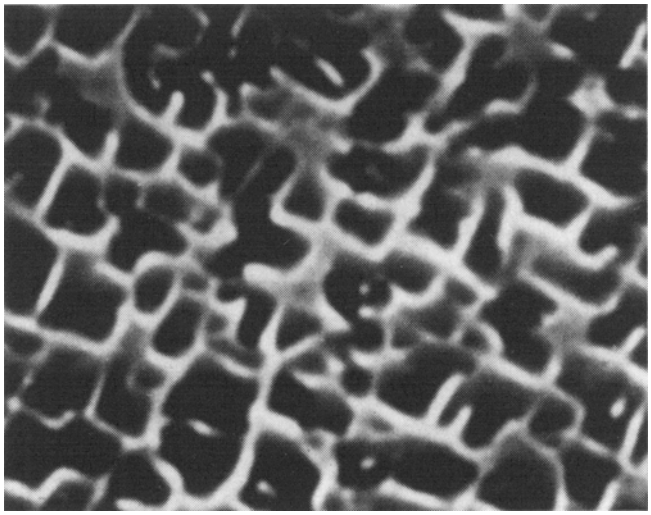

(c)

Fig. 1 Microstructures of heat-treated specimens. All at 1000×. (a) Condition A; γ' size, 0.3 μm. (b) Condition B; γ' size, 0.5 μm. (c) Condition C; 0.9 μm.

ture. The results reported in Fig. 2 and 3 indicate that both the yield and tensile strength of the material in heat-treated conditions B and C increase with temperature and reach a peak at or around 800 °C, whereas for heat-treated condition A, strength remains more or less constant up to 800 °C. Beyond this point, the yield and tensile strengths start rapidly decreasing for all three differently heat-treated materials.

The loss of yield strength after reaching a peak is typical of single-crystal nickel-based superalloys where the volume fraction of γ' is very high,[12] like the present material. Many other researchers[13,14] have reported similar phenomenon in other nickel-based superalloys. The percentage elongation values are also reported in Tables 3 to 5. It is evident from these tables that, even though the ductility has remained more or less constant at 800 °C, the strength has increased at this temperature in this material, i.e., the heat treatments (B and C) have resultant improvements in strength at high temperature (800 °C) without any loss in ductility. The tables also show that there is a decrease in ductility for all three different heat-treated materials at 650 °C. The reason is due to dynamic strain aging.[15]

As mentioned earlier, the results in Fig. 2 and 3 also indicate that both the yield and tensile strength of this material increase with an increase in temperature. It is well known that γ' has a unique characteristic, i.e., its strength increases[17] with rise in temperature. Because the present alloy contained more volume fraction of γ' (about 70%), any decrease in yield strength of the γ matrix due to rise in temperature was compensated for by an increase in yield strength of the γ'. The increased strength of γ' with temperature has been explained[16,17] by thermally activated cross slip of dislocations from {111} planes to {100} planes. This cross slip from octahedral {111} planes to cubic {100} planes occurs with increasing ease as the temperature of

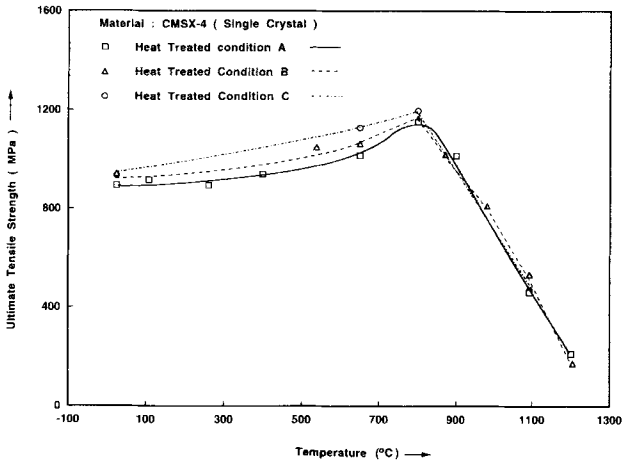

Fig. 2 Influence of temperature on ultimate tensile strength of CMSX-4.

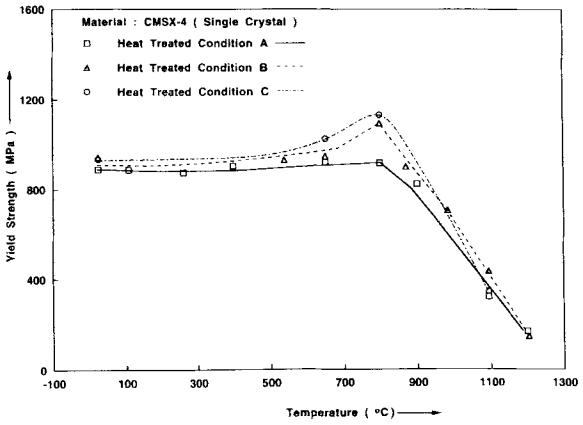

Fig. 3 Influence of temperature on yield strength of CMSX-4.

Table 3 Mechanical Properties of CMSX-4 in Heat-Treated Condition A

Temperature, °C	0.2% Yield strength, MPa	Ultimate tensile strength, MPa	Young's modulus, GPa	Elongation, %	Reduction in area, %
24	888	894	133	22.0	20.5
107	886	916	125	18.0	19.6
260	873	893	112	17.1	21.2
650	907	1031	107	13.8	17.8
800	916	1151	85	22.1	24.4
1094	321	459	80	28.8	59.5

Table 4 Mechanical Properties of CMSX-4 in Heat-Treated Condition B

Temperature, °C	Yield strength, MPa	Ultimate tensile strength, MPa	Young's modulus, GPa	Elongation, %
24	942	942	133	17.5
538	929	1049	105	12
650	947	1064	100	11.8
800	1093	1165	85	22.9
871	899	1019	84	31.8
982	704	811	82	32.9
1094	420	532	80	39.6
1204	146	172	71	39.3

Table 5 Mechanical Properties of CMSX-4 in Heat-Treated Condition C

Temperature, °C	Yield strength, MPa	Ultimate tensile strength, MPa	Elongation, %
24	934	934	24.3
650	1024	1128	7.5
800	1131	1197	26.9
1094	343	468	39.6

the material increases. Hence, an increase in strength is observed in these alloys where γ' volume fraction is relatively large as the temperature increases. Beyond 900 °C, the γ' starts rapidly dissolving and, hence, the alloy loses strength. Therefore, the strength of the alloy is lower at 1094 °C and higher temperatures.

Figures 4 to 7 report the plot of yield strength of the materials as a function of γ' size at various temperatures. Results reported in these figures indicate that with increase in γ' precipitate size, the yield strength increases in this material in the size range of the γ' studied. However, this effect is observed only up to 800 °C. At very high temperature (T = 1094 °C), there is no significant difference in yield and tensile strengths of heat-treated A, B, and C materials, i.e., the yield and tensile strengths become independent of γ' precipitate size at this temperature (1094 °C).

In nickel-based superalloys, strengthening due to presence of γ' involves coherency hardening and order hardening.[16] Coherency hardening occurs due to lattice mismatch between γ

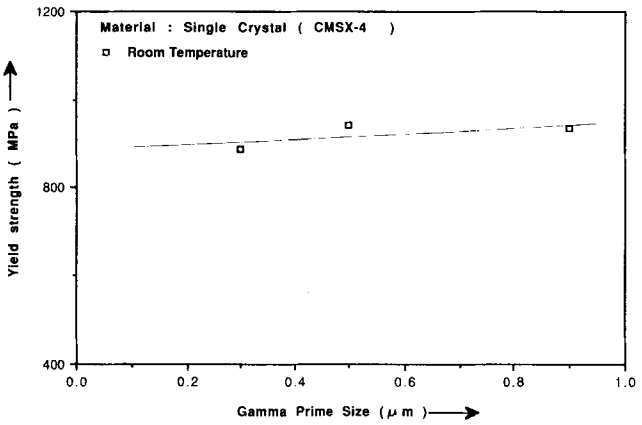

Fig. 4 Influence of γ' size on yield strength of CMSX-4 at room temperature.

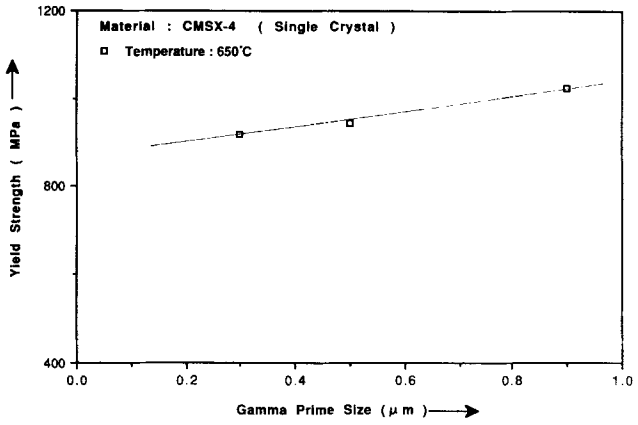

Fig. 5 Influence of γ' size on yield strength of CMSX-4 at 650 °C.

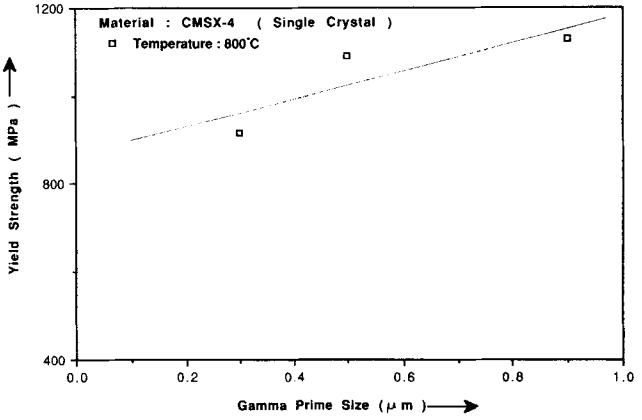

Fig. 6 Influence of γ' size on yield strength of CMSX-4 at 800 °C.

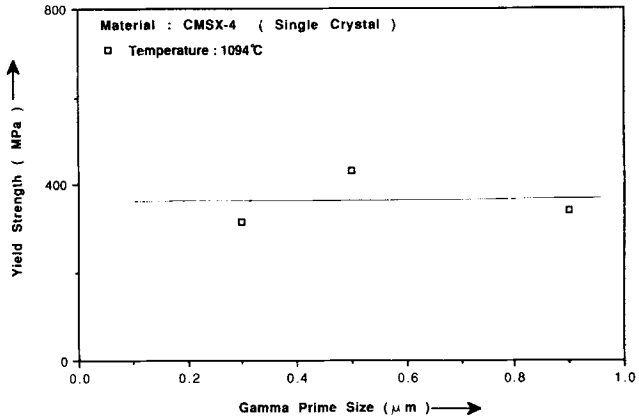

Fig. 7 Influence of γ' size on yield strength of CMSX-4 at 1094 °C.

and γ' precipitates. Order hardening, on the other hand, occurs due to the ordered LI_2 structure of the γ' phase. When a dislocation passes through this ordered γ' phase, it creates antiphase boundary (APB). Consequently, the energy required to create APB opposes the passage of dislocations, which in turn increases the strength of the material.

The increase in strength with increase in γ' precipitate size had been observed earlier by other investigators.[18,19,20] Mitchell[19] has found that strength increases as the γ' precipitate size increases. This has been attributed to the fact that when the yield strength increases with γ' precipitate size, shearing of the γ' precipitates by dislocations gives rise to increasing strength. Transmission electron microscopy (TEM) studies[15] have shown that γ' precipitates shearing by dislocations are operative up to 800 °C, whereas above 800 °C the plastic flow occurs by γ' bypass. Because the shear stress (for cutting γ' precipitates by dislocations) increases with an increase in γ' precipitate size, this results in increasing yield strength with γ' size as observed in the present material.

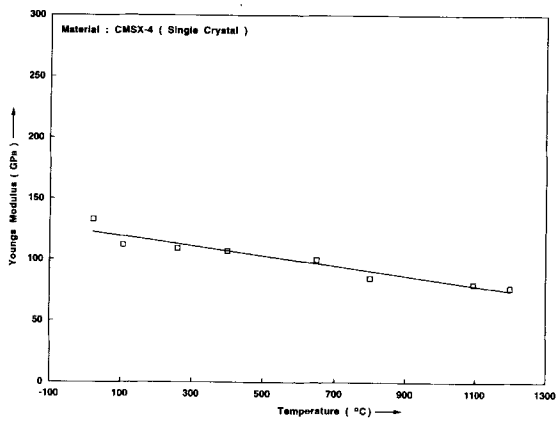

Fig. 8 Influence of temperature on Young's modulus of CMSX-4.

3.2 *Strain Hardening Exponent and Elastic Modulus*

Figure 8 is a plot of Young's modulus against temperature for CMSX-4. It is evident that the modulus of the materials decreases with rise in temperature. Interestingly, CMSX-4 maintains a higher elastic modulus at high temperature compared to other single-crystal nickel-based superalloys such as PWA 1480, etc.

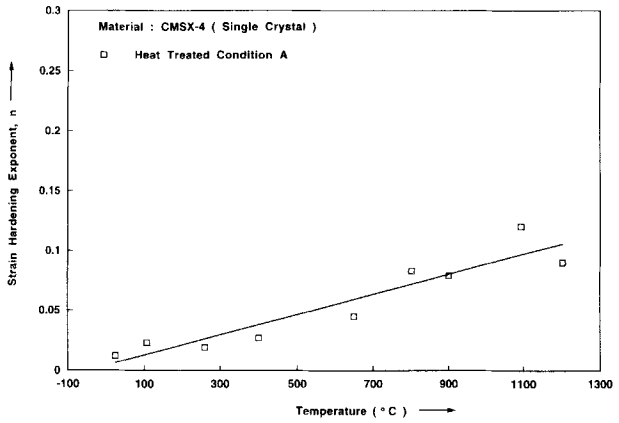

Fig. 9 Influence of temperature on strain-hardening exponent of CMSX-4 for heat-treated condition A.

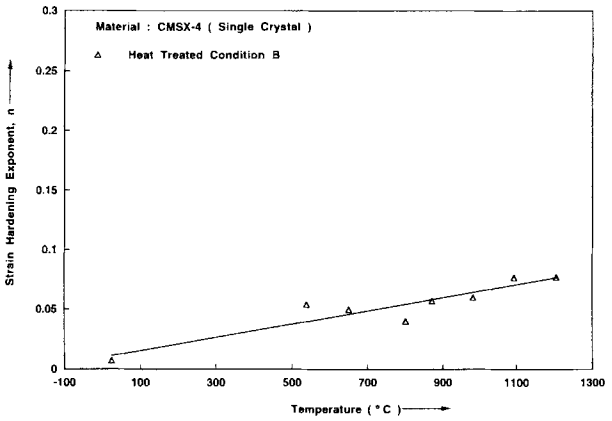

Fig. 10 Influence of temperature on strain-hardening exponent of CMSX-4 for heat-treated condition B.

Figures 9 to 11 report the influence of temperature on strain-hardening exponent, n, of these materials (A, B, and C). It is evident that strain-hardening exponent increases linearly with increase in temperature for all three different heat-treated conditions. Nickel is a face-centered cubic (fcc) material, and fcc materials are expected to have a high strain-hardening exponent. However, the present material has a very low strain-hardening exponent, as can be seen from Fig. 9 to 11. This indicates that the stacking fault energy of this alloy must be high.[21] Increase in strain-hardening exponent with temperature is indicative of the fact that more parabolic hardening must be occurring at higher temperature. Thorton et al.[16] suggested that the increase in strain-hardening rate is due to the fact that as the temperature increases, both octahedral and cubic systems start operating in this alloy. This intersection of both slip systems at higher temperature[16] creates dislocation debris and thus produces more barriers for cross slip. Preliminary studies by these authors,[21] however, indicate that more partials are present when deformed at higher temperature, indicating the presence of stacking faults in the alloy at higher temperature. These stacking faults create a barrier for cross slip, thereby decreasing plasticity. Smaller γ' size apparently promotes increasing dislocation intersection and thereby promotes stacking faults. A detailed study[21] is currently in progress to determine the concentration of partials at both room and elevated temperatures.

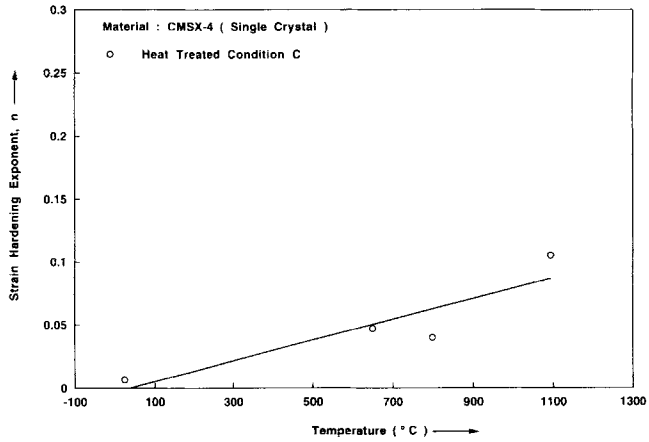

Fig. 11 Influence of temperature on strain-hardening exponent of CMSX-4 for heat-treated condition C.

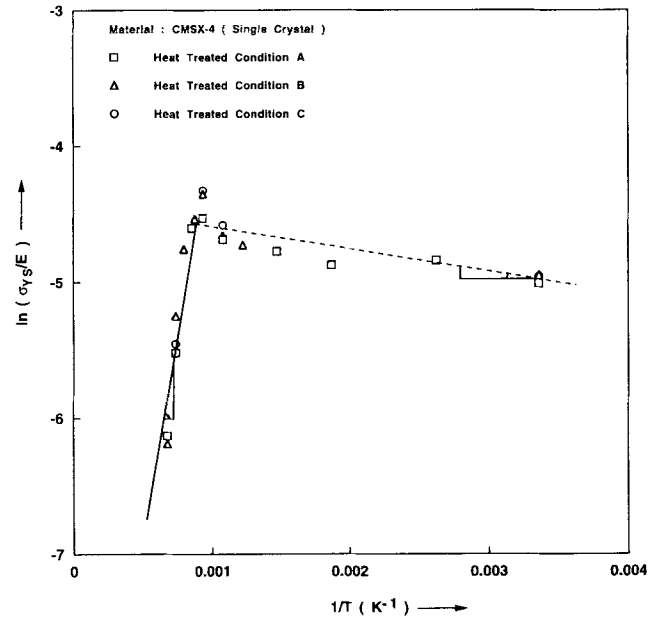

Fig. 12 A plot of modulus-normalized yield strength against inverse of temperature (Kelvin).

3.3 *Yielding Mechanism*

Because both the yield and tensile strength are dependent on the temperature as well as on the strain rate (Tables 3 and 4), plastic flow could possibly be caused by a thermally activated deformation process, and an Arrhenius type of relation might be applicable for characterizing the plastic flow behavior of this material, i.e.:

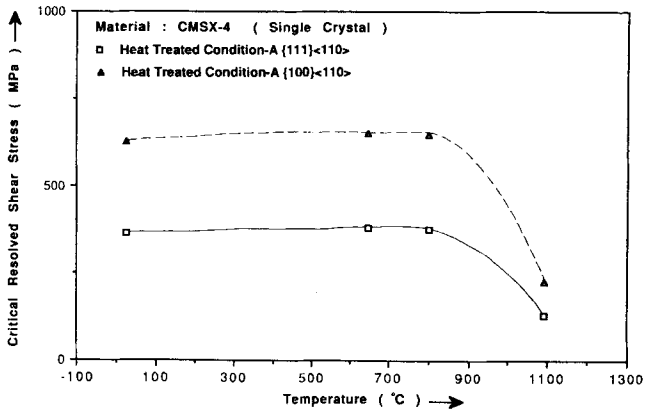

Fig. 13 Influence of temperature on critical resolved shear stress of CMSX-4 for heat-treated condition A.

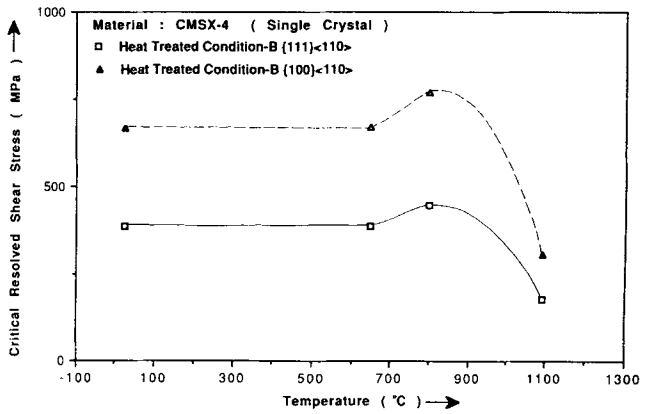

Fig. 14 Influence of temperature on critical resolved shear stress of CMSX-4 for heat-treated condition B.

Table 6 Effect of Temperature on Critical Resolved Shear Stress of CMSX-4 for Octahedral and Cubic Systems

Heat treatment	Temperature, °C	{111}⟨110⟩: Critical resolved shear stress, MPa	{100}⟨110⟩: Critical, resolved shear stress, MPa
A	24	363	682
B		384	666
C		381	660
A	650	376	651
B		386	669
C		418	724
A	800	374	648
B		446	773
C		462	779
A	1094	129	223
B		177	307

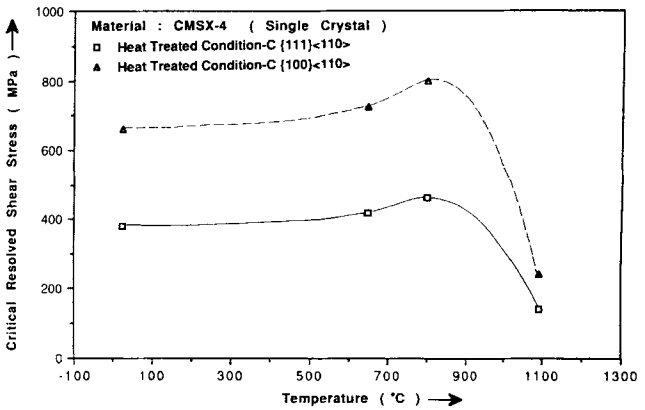

Fig. 15 Influence of temperature on critical resolved shear stress of CMSX-4 for heat-treated condition C.

$$\frac{\sigma_{ys}}{E}\text{] at constant strain and strain rate} = C \cdot \exp\frac{Q}{RT} \qquad [1]$$

Here E is the Young's modulus, Q is the activation energy for the deformation process, T is the temperature in degrees Kelvin, and R is the universal gas constant (8.314 J/mol · K). C is a material constant. In Fig. 12, the logarithmic value of the normalized value of the yield strength by Young's modulus is plotted against the inverse of temperature in degrees Kelvin (for specimens tested at strain rate of 0.005 in./in./min up to yield, and 0.05 in./in./min beyond yield). Again, each data point in this figure is averaged from three to four identical test samples. This figure indicates two distinct regions. In region I (or the high-temperature range, $T > 800$ °C), the curve has a positive slope, whereas in region II ($T < 800$ °C) the curve shows a negative slope. This indicates a change in the rate-controlling process for the deformation mechanism below and above 800 °C. The apparent activation energy of the deformation process in region I obtained from the slope of line (A) is on the order of 52 kJ/mol. The true activation energy for region I was calculated using a technique similar to that of Antolovich et al.[22] This value was found to be on the order of 520 kJ/mol, which is within the range for activation energies for self-diffusion for nickel-based superalloys at elevated temperatures. Because the activation energy for the deformation process in CMSX-4 above 800 °C (region I) was in the range of the activation energies for self-diffusion of similar nickel-based superalloys,[23,24] this indicates that yielding or plastic deformation in this alloy in region I (above 800 °C) must occur by the dislocation climb process, assisted by diffusion, i.e., the rate-controlling process for plastic flow must be γ' bypassing the dislocations. This has been verified by transmission electron microscopic studies and has been reported in another publication.[11] Below 800 °C, thermally activated hardening is occurring which is due to cross-slip process.[17]

3.4 *Influence of Temperature on Critical Resolved Shear Stress*

Preliminary studies[15] indicate that the slip planes and directions for the specimens tested at room temperature here were the primary octahedral system (111)[101]. The primary tensile axis of the specimens [001] remained constant (without rotation), apparently because of the several octahedral systems operated during the loading process. The critical resolved shear stress for these specimens were determined from the yield strength and the Schmid factor of the slip systems (octahedral

as well as cubic system) and are reported in Table 6. In Fig. 13 to 15, these critical resolved shear stresses are plotted against temperature. These plots clearly indicate the similar nature of the plot like yield and tensile strengths (Fig. 2 and 3) against temperature. Critical resolved shear stress is more or less similar for all three different γ' precipitate sizes at room temperature (within 5%), but tends to increase with γ' size at higher temperature. The critical resolved shear stress was highest at 800 °C for heat-treated conditions B and C in Fig. 14 and 15, whereas for heat-treated condition A, critical resolved shear stress is more or less constant up to 800 °C and then starts rapidly decreasing. Miner et al.[25] have also observed similar increase in critical resolved shear stress with temperature in René N4 alloy. The critical resolved shear stress was calculated for CMSX-4 based on the earlier published[26,27] models, and these values were found to be on the order of 111 and 620 MPa, respectively, at room temperature. The actual critical resolved shear stress of CMSX-4 is approximately 400 MPa at room temperature. Hence, our test results indicate that none of the above models can be used to predict the critical resolved shear stress of the present material. This difference is due to the size of γ' precipitate as well as the very high volume fraction and composition of γ' phase of the present alloy. Furthermore, both of these models ignore the contribution of lattice mismatch in strengthening. In the present alloy, due to the presence of rhenium, there is significant lattice mismatch, and this contributes significantly[9] to the strength of this alloy. There is a need to develop a new model for this material, and studies are currently in progress for developing such a model.

4. Conclusions

The yield and tensile strengths of CMSX-4 (in heat-treated conditions B and C) were found to increase with an increase in temperature up to 800 °C. Beyond this temperature, both yield and tensile strengths decrease rapidly with an increase in temperature. Both the yield and tensile strengths were found to increase with an increase in γ' precipitate size (up to 800 °C) in the size range of γ' precipitates studied in this investigation. The yield strength and temperature correlated very well by an Arrhenius-type relationship. At higher temperature (T > 800 °C), yielding was controlled by climbing process of dislocations. At lower temperatures, thermally activated hardening was taking place whereas at higher temperatures thermally activated softening occurs. The strain-hardening exponent of CMSX-4 increases with an increase in temperature. This is due to increased presence of stacking faults at higher temperature.

Acknowledgment

The authors wish to thank Mr. Robert J. Plecki, Joliet Metallurgical Laboratory, Joliet, Illinois, for his support and technical help. We are also grateful to Dr. Ken Harris of Cannon-Muskegon Corporation, Michigan, for financial support of this work.

References

1. S. Floreen, *Superalloys II*, C.T. Sims, N.S. Stoloff, and W.C. Hagel, Ed., John Wiley & Sons, 1987, p 241-290
2. D.R. Muzyka, STP 672, ASTM, 1979, p 526-546
3. C.R. Brooks, *Heat Treatment, Structure and Properties of Nonferrous Alloys*, American Society for Metals, 1982, p 139-227
4. D.N. Duhl, Single Crystal Superalloys, *Superalloys, Supercomposites, and Superceramics*, Academic Press, 1989, p 149-182
5. G.R. Leverant and B.H. Kear, *Metall. Trans. A*, Vol 1, 1970, p 491-498
6. K. Harris, G.L. Erickson, and R.E. Schwer, "Process and Alloy Optimization for CMSX-4 Superalloys Single Crystal Airfoils," Cost 501/505 Conf., High Temp. Mater. for Power Eng. (Liege, Belgium), 1990
7. K. Harris, G.L. Erickson, S.L. Sikkenga, W.D. Brentnall, J.M. Awrecoechea, and K.G. Kubarych, "Development of Two Rhenium-containing Superalloys for Single-Crystal Blade and Directionally Solidified Vane Applications in Advanced Turbine Engines," *J. Mater. Eng. Perf.*, Vol 2(No. 4), April 1993, p 481-488
8. A.F. Giamei and D.L. Anton, Rhenium Additions to a Ni-Base Superalloy: Effects of Microstructure, *Metall. Trans. A*, Vol 1 (No. 6), 1985, p 1997-2005
9. A. Sengupta and S.K. Putatunda, Kinetics of γ' Precipitation and Its Influence on Fatigue Behavior of a New Single Crystal Nickel Based Superalloy at Room Temperature, *J. Mater. Eng. Perf.*, Vol 2 (No. 1), Feb 1993, p 61-76
10. J.S. Erickson, W.A. Owezarski, and P.M. Curran, Process Speeds up Directional Solidification, *Met. Prog.*, Vol 99, 1971, p 58-66
11. "Standard Test Methods for Mechanical Testing of Metallic Materials," E-8-90, *Annual Book of ASTM Standards*, Vol 03-01, p 3-38
12. B.H. Kear and B.J. Piearcey, Tensile and Creep Properties of Single Crystals of the Nickel-Base Superalloy Mar-M 200, *Trans. AIME*, Vol. 239, Aug 1967, p 1209-1215
13. A.A. Hopgood and J.W. Martin, The Effect of Aging on the Yield Stress of a Single-Crystal Superalloy, *Mater. Sci. Eng.*, Vol 91, 1987, p 105-110
14. T.L. Lin and M. Wen, The Deformation Mechanism of a γ' *Precipitation-Hardened Nickel-Base Superalloy, Mater. Sci. Eng. A*, Vol 128, 1990, p 23-31
15. A. Sengupta, Ph.D. thesis, Wayne State University, Detroit, 1993
16. P.H. Thorton, R.G. Davies, and T.L. Johnston, The Temperature Dependence of the Flow Stress of the γ' *Phase Based upon* Ni_3Al, *Metall. Trans.*, Vol 1, 1970, p 207-218
17. B.H. Keep and H.G.F. Wilsdorf, "Dislocation Configurations in Plantically Deformed Polycrystalline Cu_3Au Alloys," *Trans. TMS-AIME*, Vol. 224, p 382, 1962
18. W.I. Mitchell, *Z.Metallkd.*, Vol 57, 1966, p 586-590
19. H. Gleiter and E. Hornbogan, Precipitation Hardening by Coherent Particles, *Mater. Sci. Eng.*, Vol 2, 1968, p 285-302
20. S.D. Antolovich and B. Lerch, *Superalloys, Supercomposites and Superceramics*, J.K. Tien and T. Caulfield, Ed., ASM International, 1989, p 365-369
21. S.K. Putatunda and A. Sengupta, unpublished data
22. W.W. Milligan and S.D. Antolovich, Yielding and Deformation Behavior of the Single Crystal Superalloy PWA 1480, *Metall. Trans. A*, Vol 18, Jan 1987, p 85-95
23. G. Jianting, D. Ranucci, E. Picco, and P.M. Strocchi, An Investigation on the Creep and Fracture Behavior of Cast Nickel-Base Superalloy IN738LC, *Metall. Trans. A*, Vol 14, Nov 1983, p 2329-2335
24. M.V. Nathal and L.J. Ebert, Elevated Temperature Creep-Rupture Behavior of the Single Crystal Nickel-Base Superalloy NASAIR 100, *Metall. Trans. A*, Vol 16, Mar 1985, p 427-439
25. R.V. Miner, R.C. Voigt, J. Gayda, and T.P. Gabb, "Orientation and Temperature Dependence of Some Mechanical Properties of the Single-crystal Nickel-base Superalloy René N_4," *Metall. Trans. A*, Vol 17, Mar 1986, p 491-496

26. B. Reppich, "Some New Aspects Concerning Particle Hardening Mechanisms in γ' Precipitating Ni-base Alloys. Pt. I: Theoretical Concept," *Acta. Metall.*, Vol 30, p 87-94, 1982

27. S.M. Copley and B.H. Kear, "A Dynamic Theory of Coherent Precipitation Hardening with Application to Nickel-base Superalloys," *Trans. AIME*, Vol 339, 1967, p 984-992